

APPLICATION OF DIFFERENTIAL QUADRATURE METHOD TO SIMULATE NATURAL CONVECTION IN A CONCENTRIC ANNULUS

C. SHU*

Department of Mechanical and Production Engineering, National University of Singapore, 10 Kent Ridge Crescent, Singapore 119260, Singapore

SUMMARY

In this paper, the Fourier expansion-based differential quadrature (FDQ) and the polynomial-based differential quadrature (PDQ) methods are applied to simulate the natural convection in a concentric annulus with a horizontal axis. The comparison and grid independence of PDQ and FDQ results are studied in detail. It was found that both PDQ and FDQ can obtain accurate numerical solutions using just a few grid points and requiring very small computational resources. It was demonstrated in the paper that the FDQ method can be applied to a periodic problem or a non-periodic problem. When FDQ is applied to a non-periodic problem (half of annulus), it can achieve the same order of accuracy as the PDQ method. And when FDQ is applied to the periodic problem (whole annulus), it is very efficient for low Rayleigh numbers. However, its efficiency is greatly reduced for the high Rayleigh numbers. The benchmark solution for $Ra = 10^2, 10^3, 3 \times 10^3, 6 \times 10^3, 10^4, 5 \times 10^4$ are also presented in the paper. Copyright © 1999 John Wiley & Sons, Ltd.

KEY WORDS: differential quadrature; annulus; Rayleigh number

1. INTRODUCTION

Natural convective heat transfer in enclosed spaces has been extensively studied due to its wide applications in engineering, such as in nuclear reactor design, cooling of electronic equipment, aircraft cabin insulation and thermal storage systems. The horizontal concentric annulus is a most commonly used geometry for these applications. The research on natural convection in a concentric annulus includes the numerical work and the experimental investigation. Among the numerical work [1–16], the low order methods, such as finite difference, finite volume and finite element methods, are usually used to make spatial discretization. In general, the low order methods need a large number of grid points to obtain accurate numerical results and thus require a lot of computational effort and virtual storage.

In seeking an efficient method using just a few grid points to obtain accurate numerical results, Bellman *et al.* [17] introduced a global method of differential quadrature (DQ). DQ approximates a derivative with respect to a co-ordinate direction at a grid point by a weighted linear sum of all the functional values in that direction. Obviously, the key to DQ is to determine the weighting coefficients for any order derivative discretization. Bellman *et al.* [17]

* Correspondence to: Department of Mechanical and Production Engineering, National University of Singapore, 10 Kent Ridge Crescent, Singapore 119260, Singapore.

suggested two ways to determine the weighting coefficients of the first-order derivative. The first way solves an algebraic equation system. The second uses a simple algebraic formulation, but with a condition that the co-ordinates of grid points should be chosen as the roots of the shifted Legendre polynomial. The early applications of DQ [17–20] usually used Bellman's first way to obtain the weighting coefficients because the co-ordinates of grid points can be chosen arbitrarily. But unfortunately, when the order of the system, i.e. the number of grid points, is large, the matrix of the system is ill-conditioned. Thus, it is very difficult to obtain the weighting coefficients using this way when the number of grid points is large. To overcome the drawbacks of DQ, Shu [21] generalized all the ways of computing the weighting coefficients under analysis of a linear vector space when the function is approximated by a high-order polynomial. As a result, the weighting coefficients of the first-order derivative are determined by a simple algebraic formulation without any restriction on choice of grid points, and the weighting coefficients of the second- and higher-order derivatives are determined by a recurrence relationship. This is a major breakthrough in the development and application of the DQ method. Since then, the DQ method has been extensively applied to solve the fluid flow problems [21–26] and the structural and vibration problems [27–42]. More recently, Shu *et al.* [43] further presented the explicit formulations to compute the weighting coefficients when the function is approximated by Fourier series expansion. For simplicity of the following discussion, the polynomial-based DQ method is noted as PDQ, while the Fourier expansion-based DQ approach is termed FDQ. It is indicated that the developed FDQ method can be applied to a periodic problem or a non-periodic problem. When a periodic problem is applied, the periodic condition is naturally considered in the FDQ formulation. Thus, no periodic condition is needed to implement in the solution process. It was shown by Shu *et al.* [43] that when a non-periodic boundary value problem is considered, the accuracy of both PDQ and FDQ results is almost the same. However, when a periodic problem is considered, the FDQ method provides much more accurate results than the PDQ method. To further study the performance of PDQ and FDO methods to periodic and non-periodic problems, the natural convection in a concentric annulus is investigated in this work. The polar system is used to solve the governing equations. In the r -direction, the flow is always a non-periodic boundary value problem, and the PDQ method will be used to discretize the derivatives, since for this case both PDQ and FDQ give almost the same result. The FDQ method is applied in the θ -direction since it can automatically treat the periodic condition. On the other hand, for the natural convection in the annulus between two concentric cylinders, the flow can be assumed to be symmetric with respect to the vertical centerlines. Thus, half of the annulus can be taken as the computational domain. Then for this case, the flow in the θ -direction becomes a non-periodic boundary value problem, and both PDQ and FDQ approaches can be applied. The performance of PDQ and FDQ methods will be validated by their application to discretize the derivatives in the θ -direction for three test cases.

2. DIFFERENTIAL QUADRATURE METHOD

For simplicity, the one-dimensional problem is chosen to demonstrate the differential quadrature method. Following the idea of an integral quadrature that uses a linear weighted summation of all the functional values to approximate an integral over a closed domain, Bellman *et al.* [17] proposed the differential quadrature (DQ) method that approximates the derivative of a smooth function at a grid point by a linear weighted summation of all the functional values in the whole computational domain. For example, the first- and second-order derivatives of $f(x)$ at a point x_i are approximated by

$$f_x(x_i) = \sum_{j=1}^N a_{ij} \cdot f(x_j), \quad \text{for } i = 1, 2, \dots, N, \quad (1)$$

$$f_{xx}(x_i) = \sum_{j=1}^N b_{ij} \cdot f(x_j), \quad \text{for } i = 1, 2, \dots, N, \quad (2)$$

where N is the number of grid points, and a_{ij} , b_{ij} are the weighting coefficients. It is noted that Equations (1) and (2) are similar except that they use different weighting coefficients. Obviously, the key procedure in DQ is to determine the weighting coefficients a_{ij} and b_{ij} . It was shown by Shu [21] and Shu *et al.* [43] that under the analysis of a linear vector space, all the ways of computing the weighting coefficients can be generalized, and when the function $f(x)$ is approximated differently, the formulation for a_{ij} and b_{ij} is also different. In the following, the respective formulations of a_{ij} and b_{ij} are presented when the function $f(x)$ is approximated by a high-order polynomial or by the Fourier series expansion.

2.1. Polynomial-based differential quadrature (PDQ)

For this case, it is supposed that the function is approximated by an $(N-1)$ th degree polynomial in the form

$$f(x) = \sum_{k=0}^{N-1} c_k \cdot x^k. \quad (3)$$

It is easy to show that the polynomial of degree less than or equal to $N-1$ constitutes an N -dimensional linear vector space V_N . From the concept of linear independence, the bases of a linear vector space can be considered as a linearly independent subset that spans the entire space. Here, if $r_k(x)$, $k = 1, 2, \dots, N$, are the base polynomials in V_N , $f(x)$ can then be expressed by

$$f(x) = \sum_{k=1}^N d_k \cdot r_k(x). \quad (4)$$

Clearly, if all the base polynomials satisfy a linear constrained relationship, such as Equation (1) or (2), so does $f(x)$. In the linear vector space, there may exist several sets of base polynomials. Each set of base polynomials can be expressed uniquely by another set of base polynomials. In computing the weighting coefficients, Shu [21] used two sets of base polynomials. The first set of base polynomials is chosen as the Lagrange interpolated polynomials

$$r_k(x) = \frac{M(x)}{(x - x_k) \cdot M^{(1)}(x_k)}, \quad (5)$$

where

$$M(x) = (x - x_1) \cdot (x - x_2) \cdot \dots \cdot (x - x_N),$$

$$M^{(1)}(x_k) = \prod_{j=1, j \neq k}^N (x_k - x_j),$$

x_1, x_2, \dots, x_N are the co-ordinates of grid points, and can be chosen arbitrarily.

Setting

$$M(x) = N(x, x_k) \cdot (x - x_k), \quad k = 1, 2, \dots, N, \quad (6)$$

with $N(x_i, x_j) = M^{(1)}(x_i) \cdot \delta_{ij}$, where δ_{ij} is the Kronecker operator, we then obtain

$$M^{(m)}(x) = N^{(m)}(x, x_k) \cdot (x - x_k) + m \cdot N^{(m-1)}(x, x_k), \quad (7)$$

for

$$m = 1, 2, \dots, N - 1; \quad k = 1, 2, \dots, N,$$

where $M^{(m)}(x)$, $N^{(m)}(x, x_k)$ are the m th-order derivative of $M(x)$ and $N(x, x_k)$.

Substituting Equation (5) into Equations (1) and (2), we obtain

$$a_{ij} = \frac{N^{(1)}(x_i, x_j)}{M^{(1)}(x_j)}, \tag{8}$$

$$b_{ij} = \frac{N^{(2)}(x_i, x_j)}{M^{(1)}(x_j)}. \tag{9}$$

Using Equation (7), Equations (8) and (9) can be further reduced to

$$a_{ij} = \frac{M^{(1)}(x_i)}{(x_i - x_j) \cdot M^{(1)}(x_j)}, \quad \text{when } j \neq i, \tag{10a}$$

$$a_{ii} = \frac{M^{(2)}(x_i)}{2M^{(1)}(x_i)}, \tag{10b}$$

$$b_{ij} = 2a_{ij} \cdot \left(a_{ii} - \frac{1}{x_i - x_j} \right), \quad \text{when } j \neq i, \tag{11a}$$

$$b_{ii} = \frac{M^{(3)}(x_i)}{3M^{(1)}(x_i)}. \tag{11b}$$

Clearly, a_{ij} , b_{ij} ($i \neq j$) can be easily computed from Equations (10a) and (11a). However, the computation of a_{ii} (Equation (10b)) and b_{ii} (Equation (11b)) involves the computation of $M^{(2)}(x_i)$ and $M^{(3)}(x_i)$, which are not easy to compute. As will be shown in the following, this difficulty can be removed by the property of the linear vector space. According to the theory of a linear vector space, one set of base polynomials can be expressed uniquely by another set of base polynomials. Thus, if one set of base polynomials satisfies a linear constrained relationship, so does another set of base polynomials. Thus, Equations (1) and (2) should also be satisfied by the second set of base polynomials x^k , $k = 0, 1, 2, \dots, N - 1$. When $k = 0$, this set of base polynomials gives

$$\sum_{j=1}^N a_{ij} = 0, \tag{12}$$

$$\sum_{j=1}^N b_{ij} = 0. \tag{13}$$

From the above equations, a_{ii} and b_{ii} can be easily determined from a_{ij} and b_{ij} ($i \neq j$). It is indicated that a recurrence relationship can also be derived to compute the weighting coefficients of higher-order derivatives. For details, see [21].

2.2. Fourier expansion-based differential quadrature (FDQ)

For this case, the function is approximated by a Fourier series expansion in the form

$$f(x) = c_0 + \sum_{k=1}^{N/2} (c_k \cos kx + d_k \sin kx). \tag{14}$$

Similar to PDQ, it is easy to show that $f(x)$ in Equation (14) constitutes an $(N + 1)$ -dimensional linear vector space with respect to the operation of addition and multiplication. If $r_k(x)$,

$k = 0, 1, \dots, N$, are the base functions, any function in the space can be expressed as a linear combination of $r_k(x)$, $k = 0, 1, \dots, N$. It is obviously observed from Equation (14) that one set of base functions is $1, \sin x, \cos x, \sin 2x, \dots, \sin(Nx/2), \cos(Nx/2)$. Similar to the PDQ approach, two sets of base functions will be used in the FDQ approach. Firstly, the Lagrange interpolated trigonometric polynomials are taken as one set of base functions:

$$r_k(x) = \frac{\sin \frac{x-x_0}{2} \cdots \sin \frac{x-x_{k-1}}{2} \cdot \sin \frac{x-x_{k+1}}{2} \cdots \sin \frac{x-x_N}{2}}{\sin \frac{x_k-x_0}{2} \cdots \sin \frac{x_k-x_{k-1}}{2} \cdot \sin \frac{x_k-x_{k+1}}{2} \cdots \sin \frac{x_k-x_N}{2}}, \quad (15)$$

for $k = 0, 1, 2, \dots, N$.

Setting

$$M(x) = \prod_{k=0}^N \sin \frac{x-x_k}{2} = N(x, x_k) \cdot \sin \frac{x-x_k}{2}, \quad (16)$$

where

$$N(x_i, x_i) = \prod_{k=0, k \neq i}^N \sin \frac{x_i-x_k}{2} = P(x_i), \quad N(x_i, x_j) = N(x_i, x_i) \cdot \delta_{ij}, \quad (17)$$

where δ_{ij} is the Kronecker operator, Equation (15) can then be reduced to

$$r_k(x) = \frac{N(x, x_k)}{P(x_k)}. \quad (18)$$

Using the same fashion as in PDQ, we let all the base functions given by Equation (18) satisfy two linear constrained relations (1) and (2). This results in the following two formulations

$$a_{ij} = \frac{N^{(1)}(x_i, x_j)}{P(x_j)}, \quad (19)$$

$$b_{ij} = \frac{N^{(2)}(x_i, x_j)}{P(x_j)}. \quad (20)$$

It is observed from Equations (19) and (20) that the computation of a_{ij} and b_{ij} is equivalent to the evaluation of $N^{(1)}(x_i, x_j)$ and $N^{(2)}(x_i, x_j)$, since $P(x_j)$ can be easily calculated by Equation (17). To evaluate $N^{(1)}(x_i, x_j)$ and $N^{(2)}(x_i, x_j)$, Equation (16) is successively differentiated to obtain

$$M^{(1)}(x) = N^{(1)}(x, x_k) \cdot \sin \frac{x-x_k}{2} + \frac{1}{2} N(x, x_k) \cdot \cos \frac{x-x_k}{2}, \quad (21)$$

$$M^{(2)}(x) = N^{(2)}(x, x_k) \cdot \sin \frac{x-x_k}{2} + N^{(1)}(x, x_k) \cdot \cos \frac{x-x_k}{2} - \frac{1}{4} N(x, x_k) \cdot \sin \frac{x-x_k}{2}, \quad (22)$$

$$M^{(3)}(x) = N^{(3)}(x, x_k) \cdot \sin \frac{x-x_k}{2} + \frac{3}{2} N^{(2)}(x, x_k) \cdot \cos \frac{x-x_k}{2} - \frac{3}{8} N^{(1)}(x, x_k) \cdot \sin \frac{x-x_k}{2} - \frac{1}{8} N(x, x_k) \cdot \cos \frac{x-x_k}{2}. \quad (23)$$

From the above equations, we can obtain the following results

$$N^{(1)}(x_i, x_j) = \frac{P(x_i)}{2 \sin \frac{x_i - x_j}{2}}, \quad \text{when } j \neq i, \quad (24)$$

$$N^{(1)}(x_i, x_i) = M^{(2)}(x_i), \quad (25)$$

$$N^{(2)}(x_i, x_j) = \frac{M^{(2)}(x_i) - N^{(1)}(x_i, x_j) \cdot \cos \frac{x_i - x_j}{2}}{\sin \frac{x_i - x_j}{2}}, \quad \text{when } j \neq i, \quad (26)$$

$$N^{(2)}(x_i, x_i) = \frac{2}{3} \left[M^{(3)}(x_i) + \frac{1}{8} N(x_i, x_i) \right]. \quad (27)$$

Substituting Equations (24) and (25) into Equation (19), we obtain

$$a_{ij} = \frac{1}{2} \cdot \frac{P(x_i)}{\sin \frac{x_i - x_j}{2} \cdot P(x_j)}, \quad \text{when } j \neq i, \quad (28)$$

$$a_{ii} = \frac{M^{(2)}(x_i)}{P(x_i)}. \quad (29)$$

Similarly, substituting Equations (26) and (27) into Equation (20) and using Equations (28) and (29), we obtain

$$b_{ij} = a_{ij} \left[2a_{ii} - \cotan \frac{x_i - x_j}{2} \right], \quad \text{when } j \neq i, \quad (30)$$

$$b_{ii} = \frac{2}{3} \left[\frac{M^{(3)}(x_i)}{P(x_i)} + \frac{1}{8} \right]. \quad (31)$$

From Equations (28) and (30), a_{ij} , b_{ij} ($i \neq j$) can be easily computed. However, the calculation of a_{ii} (Equation (29)) and b_{ii} (Equation (31)) involves the computation of $M^{(2)}(x_i)$ and $M^{(3)}(x_i)$, which are not easy to compute. This difficulty can be removed using the same manner as used in PDQ. The following two equations can be obtained by substituting the second set of base functions $1, \sin x, \cos x, \sin 2x, \dots, \sin(Nx/2), \cos(Nx/2)$ into Equations (1) and (2):

$$\sum_{j=1}^N a_{ij} = 0, \quad (32)$$

$$\sum_{j=1}^N b_{ij} = 0. \quad (33)$$

From Equations (32) and (33), a_{ii} and b_{ii} can be easily calculated from a_{ij} ($i \neq j$) and b_{ij} ($i \neq j$). It should be indicated that Equations (28), (30), (32) and (33) can be applied to the periodic problems and the non-periodic problems. For the non-periodic problems, the x range in the computational domain is $0 \leq x \leq \pi$, while for the periodic problems, the x range in the computational domain is $0 \leq x \leq 2\pi$.

3. GOVERNING EQUATIONS AND NUMERICAL DISCRETIZATION

The governing equations for the natural convection in the annulus between horizontal concentric cylinders can be written as [1]:

$$\frac{\partial U}{\partial R} + \frac{U}{R} + \frac{1}{R} \frac{\partial V}{\partial \theta} = 0, \quad (34)$$

$$\rho \frac{\partial U}{\partial t} + \rho \left[U \frac{\partial U}{\partial R} + \frac{V}{R} \frac{\partial U}{\partial \theta} - \frac{V^2}{R} \right] = - \frac{\partial P}{\partial R} + \mu \left[\frac{\partial^2 U}{\partial R^2} + \frac{1}{R} \frac{\partial U}{\partial R} + \frac{1}{R^2} \frac{\partial^2 U}{\partial \theta^2} - \frac{U}{R^2} - \frac{2}{R^2} \frac{\partial V}{\partial \theta} \right] + F_R, \quad (35)$$

$$\begin{aligned} & \rho \frac{\partial V}{\partial t} + \rho \left[U \frac{\partial V}{\partial R} + \frac{V}{R} \frac{\partial V}{\partial \theta} - \frac{UV}{R} \right] \\ &= - \frac{1}{R} \frac{\partial P}{\partial \theta} + \mu \left[\frac{\partial^2 V}{\partial R^2} + \frac{1}{R} \frac{\partial V}{\partial R} + \frac{1}{R^2} \frac{\partial^2 V}{\partial \theta^2} - \frac{V}{R^2} + \frac{2}{R^2} \frac{\partial U}{\partial \theta} \right] + F_\theta, \end{aligned} \quad (36)$$

$$\rho \frac{\partial T}{\partial t} + \rho c \left[U \frac{\partial T}{\partial R} + \frac{V}{R} \frac{\partial T}{\partial \theta} \right] = k \left[\frac{\partial^2 T}{\partial R^2} + \frac{1}{R} \frac{\partial T}{\partial R} + \frac{1}{R^2} \frac{\partial^2 T}{\partial \theta^2} \right], \quad (37)$$

where the co-ordinate R is measured from the center of the system, and θ is measured clockwise from the upward vertical line. The radial velocity U is positive radially outwards, the angular velocity V is positive in the clockwise direction. F_R and F_θ are the body force components in the radial and angular directions respectively, which can be written as functions of the temperature difference:

$$F_R = g\rho\beta(T - T_o) \cos \theta, \quad (38a)$$

$$F_\theta = g\rho\beta(T - T_o) \sin \theta, \quad (38b)$$

where g is the gravitational acceleration, T the temperature at a point within the fluid, T_o the temperature of the outer cylinder and β the thermal volumetric expansion coefficient. For the two-dimensional problem, the use of vorticity–streamfunction formulation can simplify the solution procedure. With the streamfunction, the velocity components U and V can be expressed as

$$U = \frac{1}{R} \frac{\partial \Psi}{\partial \theta}, \quad V = - \frac{\partial \Psi}{\partial R}.$$

Furthermore, by setting

$$\psi = \frac{\Psi}{\alpha}, \quad r = \frac{R}{L}, \quad \phi = \frac{T - T_o}{T_i - T_o}, \quad u = \frac{UL}{\alpha}, \quad v = \frac{VL}{\alpha}, \quad t = \frac{\bar{t}\alpha}{L^2},$$

where $\alpha = k/\rho c$ is the thermal diffusivity, L is the gap between the cylinders and T_i is the temperature of the inner cylinder, Equations (34)–(37) can be simplified as

$$\nabla^2 \psi = -\omega, \quad (39)$$

$$\frac{1}{Pr} \frac{\partial \omega}{\partial t} + \frac{1}{Pr} \left[u \frac{\partial \omega}{\partial r} + \frac{v}{r} \frac{\partial \omega}{\partial \theta} \right] = \nabla^2 \omega - Ra \left[\sin \theta \frac{\partial \phi}{\partial r} + \frac{1}{r} \cos \theta \frac{\partial \phi}{\partial \theta} \right], \quad (40)$$

$$\frac{\partial \phi}{\partial t} + u \frac{\partial \phi}{\partial r} + \frac{v}{r} \frac{\partial \phi}{\partial \theta} = \nabla^2 \phi, \quad (41)$$

where

$$\nabla^2 = \frac{\partial^2}{\partial r^2} + \frac{1}{r} \frac{\partial}{\partial r} + \frac{1}{r^2} \frac{\partial^2}{\partial \theta^2}$$

is a Laplacian operator.

The dimensionless parameters appearing in the Equations (39)–(41) are the Prandtl number $Pr = \mu c/k$ and the Rayleigh number $Ra = \rho g \beta L^3 (T_i - T_o) / \mu \alpha$.

For the natural convection in an annulus between two concentric cylinders, the flow is symmetric with respect to the vertical centerline. Thus, half of the annulus can be taken as the computational domain. This can be the case when the PDQ or FDQ method with a non-periodic condition is applied in the θ -direction. However, when the FDQ method with a periodic condition is used in the θ -direction, the whole annulus should be chosen as the computational domain. The boundary conditions on two impermeable isothermal walls are given by

$$\psi = u = v = 0, \quad \omega = -\frac{\partial^2 \psi}{\partial r^2}, \quad \phi = 1, \quad (42)$$

on the inner cylinder and

$$\psi = u = v = 0, \quad \omega = -\frac{\partial^2 \psi}{\partial r^2}, \quad \phi = 0 \quad (43)$$

on the outer cylinder. When half of the annulus is taken as the computational domain, the following symmetric condition is applied along two vertical lines of symmetry at $\theta = 0$ and $\theta = \pi$:

$$\psi = v = \omega = \frac{\partial u}{\partial \theta} = \frac{\partial \phi}{\partial \theta} = 0. \quad (44)$$

When the whole annulus is taken as the computational domain, the periodic condition is required in the θ -direction, which can be naturally implemented by the FDQ method.

In the present study, the spatial derivatives in the r -direction are discretized by the PDQ method, while in the θ -direction the derivatives will be discretized by either the PDQ or the FDQ method. After spatial discretization by PDQ or FDQ, Equations (39)–(41) can be reduced to

$$\sum_{k=1}^N \frac{b_{i,k}}{r_j^2} \cdot \psi_{k,j} + \sum_{k=1}^M \left(\frac{\bar{a}_{j,k}}{r_j} + \bar{b}_{j,k} \right) \cdot \psi_{i,k} = -\omega_{i,j}, \quad (45)$$

$$\begin{aligned} & \frac{1}{Pr} \frac{d\omega_{i,j}}{dt} + \frac{1}{Pr} \left[u_{i,j} \sum_{k=1}^M \bar{a}_{j,k} \cdot \omega_{i,k} + \frac{v_{i,j}}{r_j} \sum_{k=1}^N a_{i,k} \cdot \omega_{k,j} \right] \\ & = \sum_{k=1}^N \frac{b_{i,k}}{r_j^2} \cdot \omega_{k,j} + \sum_{k=1}^M \left(\frac{\bar{a}_{j,k}}{r_j} + \bar{b}_{j,k} \right) \cdot \omega_{i,k} - Ra \left[\sin \theta_i \sum_{k=1}^M \bar{a}_{j,k} \cdot \phi_{i,k} + \frac{\cos \theta_i}{r_j} \sum_{k=1}^N a_{i,k} \cdot \phi_{k,j} \right], \end{aligned} \quad (46)$$

$$\frac{d\phi_{i,j}}{dt} + u_{i,j} \sum_{k=1}^M \bar{a}_{j,k} \cdot \phi_{i,k} + \frac{v_{i,j}}{r_j} \sum_{k=1}^N a_{i,k} \cdot \phi_{j,k} = \sum_{k=1}^N \frac{b_{i,k}}{r_j^2} \cdot \phi_{k,j} + \sum_{k=1}^M \left(\frac{\bar{a}_{j,k}}{r_j} + \bar{b}_{j,k} \right) \cdot \phi_{i,k}, \quad (47)$$

where $i = 1, 2, \dots, N$; $j = 1, 2, \dots, M$; $a_{i,k}$, $b_{i,k}$ are the weighting coefficients of the first- and second-order derivatives in the θ -direction; $\bar{a}_{i,k}$, $\bar{b}_{i,k}$ are the weighting coefficients of the first- and second-order derivatives in the r -direction. When the PDQ method is applied, the weighting coefficients are computed from Equations (10a), (11a), (12) and (13), while for the application of the FDQ method, the weighting coefficients are calculated from Equations (28), (30), (32) and (33). Similar to the discretization of governing equations, the derivatives in the boundary conditions can also be discretized by the PDQ or FDQ method.

4. RESULTS AND DISCUSSION

As mentioned above, the PDQ method is used to discretize derivatives in the r -direction. The performance and comparison of PDQ and FDQ methods are studied by their application in the θ -direction. Since the computational domain can be either taken as half of the annulus or the whole annulus, three cases for this study will follow

Case 1:

Half of the annulus is considered as the computational domain and the PDQ method is applied in the θ -direction;

Case 2:

Half of the annulus is taken as the computational domain and the FDQ method is applied in the θ -direction;

Case 3:

The whole annulus is considered as the computational domain and the FDQ method is applied in the θ -direction.

For the convenience of the following discussion, the results of case 1 are noted as PDQ, the results of case 2 are termed as FDQNP, and the results of case 3 are represented by FDQP. In the r -direction, the co-ordinates of grid points are chosen as

$$r_j = \frac{1}{RR-1} + \frac{1 - \cos\left(\frac{j-1}{M-1} \cdot \pi\right)}{2}, \quad j = 1, 2, \dots, M, \quad (48)$$

where $RR = R_o/R_i$ is the ratio of radius, R_i, R_o are the inner and outer cylinder radii respectively.

In the θ -direction, the co-ordinates of grid points are chosen as

$$\theta_i = \frac{\pi}{2} \left[1 - \cos\left(\frac{i-1}{N-1} \cdot \pi\right) \right], \quad i = 1, 2, \dots, N \quad (49)$$

for cases 1 and 2, and

$$\theta_i = 2\pi \frac{i-1}{N}, \quad i = 1, 2, \dots, N \quad (50)$$

for case 3.

It is noted that for cases 1 and 2, the symmetric boundary condition (44) should be implemented at $\theta = 0$ and $\theta = \pi$. However, for case 3, since the periodic condition is naturally considered in the FDQ formulation, no boundary condition is needed to implement in the θ -direction.

In the present work, the Euler implicit scheme is applied to discretize the time derivative in the vorticity and temperature equations, and the resultant algebraic equations are solved by the SOR method. The computed values of average equivalent conductivities are used to compare the PDQ, FDQNP and FDQP results, and to study the convergence (grid independence) of numerical results. The average equivalent conductivity is defined as

$$\bar{k}_{\text{eq}} = \frac{-\ln(RR)}{2\pi} \oint \frac{\partial \phi}{\partial n} \cdot ds. \quad (51)$$

Table I. Convergence of computed average equivalent conductivities for $Ra = 10^2$

Mesh size ($\theta \times r$)	Inner cylinder, \bar{k}_{eq_i}			Outer cylinder, \bar{k}_{eq_o}		
	PDQ	FDQNP	FDQP	PDQ	FDQNP	FDQP
3×5	0.993	0.985	0.994	0.993	0.985	0.994
3×7	1.000	0.991	1.001	1.000	0.991	1.002
3×8	1.000	0.992	1.001	1.000	0.992	1.001
3×9	1.000	0.992	1.001	1.000	0.992	1.001
5×8	1.001	1.001	1.001	1.001	1.001	1.001
Kuehn and Glodstein [1]		1.000			1.002	

The above equation can be further reduced to

$$\bar{k}_{eq_i} = \frac{-\ln(RR)}{2\pi(RR-1)} \int_0^{2\pi} \frac{\partial \phi}{\partial r} \cdot d\theta \quad (52a)$$

for the inner cylinder, and

$$\bar{k}_{eq_o} = -\frac{RR \cdot \ln(RR)}{2\pi(RR-1)} \int_0^{2\pi} \frac{\partial \phi}{\partial r} \cdot d\theta \quad (52b)$$

for the outer cylinder. For all the computations, Pr and L/D_i are set as 0.7 and 0.8 respectively, and the converged solutions are obtained when the maximum absolute value of residuals of vorticity, temperature and streamfunction equations are less than 10^{-3} .

The average equivalent conductivities computed by PDQ, FDQNP and FDQP methods for $Ra = 10^2, 10^3, 3 \times 10^3, 6 \times 10^3, 10^4, 5 \times 10^4$ are listed in Tables I, II, III, IV, V and VI. Also included in these tables are the results of Kuehn and Goldstein [1] obtained from the second-order finite difference scheme. The PDQ, FDQNP and FDQP results are obtained by using different mesh sizes. It can be observed from the tables that for all the cases, the convergence of PDQ, FDQNP and FDQP results is very good. For the given Rayleigh number, when the mesh size is above a certain grid, the numerical solution is independent of mesh size, and the computed average equivalent conductivities for the inner and outer cylinders are the same. This confirms the theoretical analysis. Since there is no energy loss in the whole system, the theoretical average equivalent conductivities for the inner and outer cylinders should be the same. From this computation, it is believed that the accurate values of

Table II. Convergence of computed average equivalent conductivities for $Ra = 10^3$

Mesh size ($\theta \times r$)	Inner cylinder, \bar{k}_{eq_i}			Outer cylinder, \bar{k}_{eq_o}		
	PDQ	FDQNP	FDQP	PDQ	FDQNP	FDQP
3×9	1.000	0.992	1.068	1.000	0.992	1.068
5×9	1.083	1.086	1.082	1.084	1.086	1.082
7×9	1.081	1.082	1.082	1.082	1.082	1.082
8×9	1.082	1.082	1.082	1.082	1.082	1.082
5×11	1.084	1.086	1.082	1.085	1.086	1.082
5×8	1.082	1.084	1.081	1.088	1.089	1.085
Kuehn and Glodstein [1]		1.081			1.084	

Table III. Convergence of computed average equivalent conductivities for $Ra = 3 \times 10^3$

Mesh size ($\theta \times r$)	Inner cylinder, k_{eq_i}			Outer cylinder, \bar{k}_{eq_o}		
	PDQ	FDQNP	FDQP	PDQ	FDQNP	FDQP
5×13	1.431	1.488	1.404	1.436	1.488	1.404
9×13	1.396	1.396	1.396	1.396	1.397	1.396
13×13	1.397	1.397	1.397	1.397	1.397	1.397
15×13	1.397	1.397	1.397	1.397	1.397	1.397
13×15	1.397	1.397	1.397	1.397	1.397	1.397
13×11	1.397	1.397	1.397	1.396	1.396	1.396
Kuehn and Glodstein [1]		1.404			1.402	

average equivalent conductivity are 1.001, 1.082, 1.397, 1.715, 1.979 and 2.958 for $Ra = 10^2$, 10^3 , 3×10^3 , 6×10^3 , 10^4 , 5×10^4 respectively. And these values can be considered as the benchmark solutions for the respective Rayleigh numbers that are summarized in Table VII.

Since the PDQ method is applied in the r -direction for all the cases, the minimum number of mesh points required in the r -direction for a grid-independent solution is the same for PDQ, FDQNP and FDQP results. It can be seen from Tables I, II, III, IV, V and VI that the minimum number of mesh points required for a grid-independent solution in the r -direction is 8, 9, 13, 15, 15 and 21 respectively for $Ra = 10^2$, 10^3 , 3×10^3 , 6×10^3 , 10^4 , 5×10^4 . In the θ -direction, three approaches are used. Thus, the minimum number of mesh points required in the θ -direction for a grid-independent solution is different for PDQ, FDQNP and FDQP results. For the convenience of the following discussion, the minimum number of mesh points for a grid-independent solution in the θ -direction is noted as 'the minimum number of mesh points'. It was found that the FDQP method is very efficient for low Rayleigh numbers. It can be seen from Table I that when $Ra = 10^2$, PDQ and FDQNP require five mesh points in the range of $0 \leq \theta \leq 180^\circ$, while FDQP needs only three mesh points in the range of $0 \leq \theta \leq 360^\circ$ to obtain a grid-independent solution. Table II shows that when $Ra = 10^3$, the minimum number of mesh points is increased to 8, 7 and 5 respectively for PDQ, FDQNP and FDQP results. When $Ra = 3 \times 10^3$, the minimum number of mesh points is the same for PDQ, FDQNP and FDQP results, and is increased to 13. This can be observed in Table III. Table IV demonstrates that when $Ra = 6 \times 10^3$, the minimum number of mesh points for FDQP results is larger than that for PDQ results. For this case, the minimum number of mesh points

Table IV. Convergence of computed average equivalent conductivities for $Ra = 6 \times 10^3$

Mesh size ($\theta \times r$)	Inner cylinder, \bar{k}_{eq_i}			Outer cylinder, \bar{k}_{eq_o}		
	PDQ	FDQNP	FDQP	PDQ	FDQNP	FDQP
11×15	1.716	1.716	1.712	1.720	1.717	1.712
15×15	1.715	1.716	1.716	1.715	1.716	1.716
17×15	1.715	1.715	1.715	1.715	1.715	1.715
19×15	1.715	1.715	1.715	1.715	1.715	1.715
17×17	1.715	1.715	1.715	1.715	1.715	1.715
17×13	1.716	1.716	1.716	1.715	1.715	1.715
Kuehn and Glodstein [1]		1.736			1.735	

Table V. Convergence of computed average equivalent conductivities for $Ra = 10^4$

Mesh size ($\theta \times r$)	Inner cylinder, \bar{k}_{eq_i}			Outer cylinder, \bar{k}_{eq_o}		
	PDQ	FDQNP	FDQP	PDQ	FDQNP	FDQP
15×15	1.980	1.980	1.984	1.979	1.980	1.983
17×15	1.979	1.980	1.981	1.979	1.979	1.981
19×15	1.979	1.979	1.980	1.979	1.979	1.980
19×17	1.979	1.979	1.980	1.979	1.979	1.980
27×15	1.979	1.979	1.979	1.979	1.979	1.979
19×13	1.981	1.981	1.981	1.979	1.979	1.979
Kuehn and Glodstein [1]		2.010			2.005	

is 15, 17 and 17 respectively for PDQ, FDQNP and FDQP results. When the Rayleigh number is high, the efficiency of FDQP method is greatly reduced. This can be noticed in Tables V and VI. Table V shows that when $Ra = 10^4$, PDQ and FDQNP methods need 17 and 19 mesh points, while FDQP method requires 27 mesh points to get a grid-independent solution. From Table VI, it can be seen that when Ra is further increased to 5×10^4 , the minimum number of mesh points is increased to 29, 29 and 49 respectively for PDQ, FDQNP and FDQP results. Clearly, the minimum number of mesh points for FDQP results is increased much faster than for PDQ and FDQNP results. However, if we consider the number of mesh points used in the half of annulus, we can find that the number of mesh points used for FDQP results is still less than that for PDQ and FDQNP results. Although in the above discussion, the minimum number of mesh points is studied for a grid-independent solution, the reasonable numerical results can be obtained by using much smaller mesh sizes. This can be observed in Tables I, II, III, IV, V and VI. Since accurate PDQ, FDQNP and FDQP results are obtained by very small mesh sizes, the required computational time is tiny, especially for the low Rayleigh number flows. Table VIII lists the iteration numbers and the computation time (s) required on LEONIS for a grid-independent solution of $Ra = 10^2, 10^3, 3 \times 10^3, 6 \times 10^3, 10^4, 5 \times 10^4$. It can be seen from Table VIII that when $Ra \leq 3 \times 10^3$, all three methods require less than 1 s computation time to get a grid-independent solution. As the Rayleigh number increases, the required computation time also increases. For all the cases studied, the required computation time for a grid-independent solution is less than 2 min. It can also be observed from Table VIII that the FDQP method usually needs less iterations than the PDQ and FDQNP methods to

Table VI. Convergence of computed average equivalent conductivities for $Ra = 5 \times 10^4$

Mesh size ($\theta \times r$)	Inner cylinder, \bar{k}_{eq_i}			Outer cylinder, \bar{k}_{eq_o}		
	PDQ	FDQNP	FDQP	PDQ	FDQNP	FDQP
19×21	2.958	2.958	2.994	2.960	2.956	2.994
25×21	2.958	2.958	2.986	2.957	2.957	2.986
29×21	2.958	2.958	2.965	2.958	2.958	2.965
31×21	2.958	2.958	2.963	2.958	2.958	2.963
49×21	2.958	2.958	2.958	2.958	2.958	2.958
29×19	2.958	2.958	2.965	2.956	2.956	2.966
Kuehn and Glodstein [1]		3.024			2.973	

Table VII. Benchmark solution of average equivalent conductivities

Equivalent conductivities	Ra					
	10^2	10^3	3×10^3	6×10^3	10^4	5×10^4
Inner cylinder \bar{k}_{eq_i}	1.001	1.082	1.397	1.715	1.979	2.958
Outer cylinder \bar{k}_{eq_o}	1.001	1.082	1.397	1.715	1.979	2.958

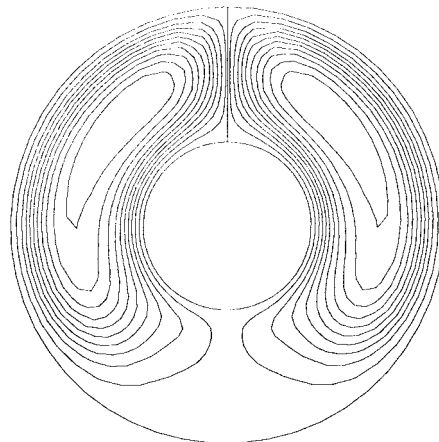
get a converged solution. However, it requires more operation time per iteration than other two methods. Among PDQ and FDQNP methods, PDQ requires less operation time per iteration. It was found that for all the cases, the flow patterns obtained from PDQ, FDQNP and FDQP methods are the same. Figure 1 shows the streamlines and the isotherms of FDQP results for $Ra = 5 \times 10^4$. The separation of inner and outer cylinder thermal boundary layer and the symmetry of flow pattern can be seen clearly.

5. CONCLUSIONS

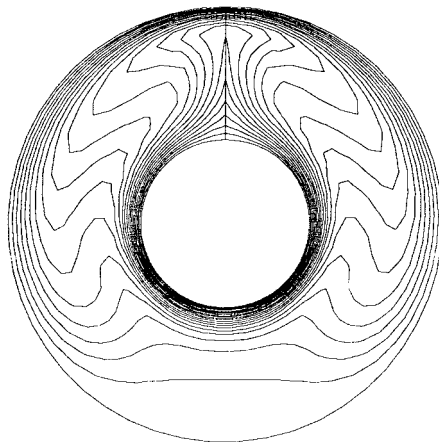
The polynomial-based differential quadrature (PDQ) and the Fourier expansion-based differential quadrature (FDQ) are applied in this study to simulate the natural convection in an annulus between two concentric cylinders. It was found that the FDQ method can be applied to a periodic or a non-periodic problem. When FDQ is applied in the half of annulus (non-periodic problem), it can achieve the same order of accuracy as the PDQ method. And when FDQ is applied in the whole annulus (periodic problem), it is very efficient for low

Table VIII. Iterations and computation time required for a grid-independent solution

Ra	Methods	Mesh sizes	Iterations	Run time (s)
10^2	PDQ	5×8	103	0.09
	FDQNP	5×8	109	0.10
	FDOP	3×8	85	0.07
10^3	PDQ	8×9	172	0.15
	FDQNP	7×9	162	0.16
	FDOP	5×9	126	0.11
3×10^3	PDQ	13×13	427	0.75
	FDQNP	13×13	411	0.83
	FDOP	13×13	349	0.81
6×10^3	PDQ	15×15	529	1.45
	FDQNP	17×15	629	2.16
	FDOP	17×15	395	1.55
10^4	PDQ	17×15	544	1.71
	FDQNP	19×15	566	2.42
	FDQP	27×15	552	4.51
5×10^4	PDQ	29×21	3596	41.68
	FDQNP	29×21	3502	40.61
	FDQP	49×21	3331	96.12



(a) Streamlines



(b) Isotherms

Figure 1. Streamlines and isotherms of FDQP for $Ra = 5 \times 10^4$.

Rayleigh number flows. However, its efficiency is greatly reduced for the high Rayleigh number flows. For this case, it is suggested to take half of the annulus as the computational domain in order to save computational effort. For all the cases, PDQ and FDQ can obtain accurate numerical results by using a considerably small number of grid points and requiring tiny computation time. The benchmark solutions for $Ra = 10^2, 10^3, 3 \times 10^3, 6 \times 10^3, 10^4, 5 \times 10^4$ are also presented in the paper.

APPENDIX A. NOMENCLATURE

a_{ij}, b_{ij}	weighting coefficients of the first- and second-order derivatives in θ -direction
$\bar{a}_{ij}, \bar{b}_{ij}$	weighting coefficients of the first- and second-order derivatives in r -direction
c	specific heat at constant pressure
D_i	diameter of inner cylinder

f_x, f_{xx}	first- and second-order derivatives of f with respect to x
g	acceleration due to gravity
k	thermal conductivity
\bar{k}_{eq}	average equivalent conductivity
\bar{k}_{eq_i}	average equivalent conductivity of inner cylinder
\bar{k}_{eq_o}	average equivalent conductivity of outer cylinder
L	gap of annulus, $L = R_o - R_i$
M	number of mesh points in r -direction
N	number of mesh points in θ -direction
P	pressure
Pr	Prandtl number
Ra	Rayleigh number
R_i	radius of inner cylinder
R_o	radius of outer cylinder
RR	radius ratio, $RR = R_o/R_i$
R	radial co-ordinate
r	dimensionless radial co-ordinate
T	temperature
T_i, T_o	temperatures of inner and outer cylinders
U, V	velocity components in R -, θ -directions
u, v	dimensionless velocity components in r -, θ -directions

Greek letters

α	thermal diffusivity
β	thermal expansion coefficient
ϕ	dimensionless temperature,
θ	angular co-ordinate
μ	viscosity
ν	kinematic viscosity
ρ	density
ω	vorticity
ψ	dimensionless streamfunction

REFERENCES

1. T.H. Kuehn and R.J. Glodstein, 'An experimental and theoretical study of natural convection in the annulus between horizontal concentric cylinders', *J. Fluid Mech.*, **74**, 695–719 (1976).
2. U. Projahn, H. Reiger and H. Beer, 'Numerical analysis of laminar natural convection between concentric and eccentric cylinders', *Numer. Heat Transf.*, **4**, 131–146 (1981).
3. R.D. Boyd, 'Unified theory for correlating steady laminar natural convection heat transfer data from horizontal annuli', *Int. J. Heat Mass Transf.*, **24**, 1545–1548 (1981).
4. B. Farouk and S.I. Guceri, 'Laminar and turbulent natural convection in the annulus between horizontal concentric cylinders', *ASME J. Heat Transf.*, **104**, 631–636 (1982).
5. M.A. Hessami, P. Hollard, R.D. Rowe and D.W. Ruth, 'Study of free convective heat transfer in a horizontal annulus with a large radii ratio', *ASME J. Heat Transf.*, **107**, 603–610 (1985).
6. A.O. Niecele and S.V. Patankar, 'Laminar mixed convection in a concentric annulus with horizontal axis', *ASME J. Heat Transf.*, **107**, 902–909 (1985).
7. E.K. Glakpe, C.B. Watkinsand and J.N. Cannon, 'Constant heat flux solutions for natural convection between concentric and eccentric horizontal cylinders', *Numer. Heat Transf.*, **10**, 279–295 (1986).

8. S.V. Randriamampianina, A.P. Bontoux and B. Roux, 'Boundary driven flows in rotating cylindrical annulus', *Int. J. Heat Mass Transf.*, **30**, 1275–1286 (1987).
9. E.H. Bishop, 'Heat transfer by natural convection of helium between horizontal isothermal concentric cylinders at cryogenic temperatures', *ASME J. Heat Transf.*, **110**, 109–115 (1988).
10. T.S. Lee, 'Laminar fluid convection between concentric and eccentric heated horizontal rotating cylinders for low Prandtl number fluids', *Int. J. Numer. Methods Fluids*, **14**, 1037–1062 (1991).
11. I. Pop, D.B. Ingham and P. Cheng, 'Transient natural convection in a horizontal concentric annulus filled with a porous medium', *ASME J. Heat Transf.*, **114**, 990–997 (1992).
12. J.C. Chai and S.V. Patankar, 'Laminar natural convection in internally finned horizontal annuli', *Numer. Heat Transf.*, **24**, 67–87 (1993).
13. Y. Miki, K. Fukuda and N. Taniguchi, 'Large eddy simulation of turbulent natural convection in concentric horizontal annuli', *Int. J. Heat Fluid Flow*, **14**, 210–216 (1993).
14. J.S. Yoo, C.J. Young and M.U. Kim, 'Multicellular natural convection of a low Prandtl number fluid between horizontal concentric cylinders', *Numer. Heat Transf.*, **25**, 103–115 (1994).
15. J. Sarr, C. Mbow, H. Chehouani, B. Zeghmami, S. Benet and M. Daguinet, 'Study of natural convection in an enclosure bounded by two concentric cylinders and two diametric planes', *ASME J. Heat Transf.*, **117**, 130–137 (1995).
16. F. Moukalled and S. Acharya, 'Natural convection in the annulus between concentric horizontal circular and square cylinders', *J. Thermophys. Heat Transf.*, **10**, 524–531 (1996).
17. R. Bellman, B.G. Kashaf and J. Casti, 'Differential quadrature: A technique for the rapid solution of non-linear partial differential equations', *J. Comput. Phys.*, **10**, 40–52 (1972).
18. S.K. Jang, C.W. Bert and A.G. Striz, 'Application of differential quadrature to static analysis of structural components', *Int. J. Numer. Method Eng.*, **28**, 561–577 (1989).
19. J.O. Mingle, 'The method of differential quadrature for transient non-linear diffusion', *J. Math. Anal. Appl.*, **60**, 559–569 (1977).
20. F. Civan and C.M. Sliepcevich, 'Differential quadrature for multidimensional problems', *J. Math. Anal. Appl.*, **101**, 423–443 (1984).
21. C. Shu, 'Generalized differential–integral quadrature and application to the simulation of incompressible viscous flows including parallel computation', *Ph.D. Thesis*, University of Glasgow, July 1991.
22. C. Shu and B.E. Richards, 'Application of generalized differential quadrature to solve two-dimensional incompressible Navier–Stokes equations', *Int. J. Numer. Methods Fluids*, **15**, 791–798 (1992).
23. C. Shu and B.E. Richards, 'Parallel simulation of incompressible viscous flows by generalized differential quadrature', *Comput. Syst. Eng.*, **3**, 271–281 (1992).
24. C. Shu, Y.T. Chew and B.E. Richards, 'Generalized differential and integral quadrature and their application to solve boundary layer equations', *Int. J. Numer. Methods Fluids*, **21**, 723–733 (1995).
25. C. Shu, Y.T. Chew, B.C. Khoo and K.S. Yeo, 'Solutions of three-dimensional boundary layer equations by global methods of generalized differential–integral quadrature', *Int. J. Numer. Methods Heat Fluid Flow*, **6**, 61–75 (1995).
26. C. Shu, B.C. Khoo, Y.T. Chew and K.S. Yeo, 'Numerical studies of unsteady boundary layer flows past an impulsively started circular cylinder by GDQ and GIQ approaches', *Comput. Methods Appl. Mech. Eng.*, **135**, 229–241 (1996).
27. C.W. Bert, X. Wang and A.G. Striz, 'Differential quadrature for static and free vibration analysis of anisotropic plates', *Int. J. Solids Struct.*, **30**, 1737–1744 (1993).
28. P.A.A. Laura and R.H. Gutierrez, 'Analysis of vibrating Timoshenko beams using the method of differential quadrature', *Shock Vib.*, **1**, 89–93 (1993).
29. P.A.A. Laura and R.H. Gutierrez, 'Analysis of vibrating rectangular plates with non-uniform boundary conditions by using the differential quadrature method', *J. Sound Vib.*, **173**, 702–706 (1994).
30. C.W. Bert, X. Wang and A.G. Striz, 'Static and free vibrational analysis of beams and plates by differential quadrature method', *Acta Mech.*, **102**, 11–24 (1994).
31. H. Du, M.K. Lim and R.M. Lin, 'Application of generalized differential quadrature method to structural problems', *Int. J. Numer. Methods Eng.*, **37**, 1881–1896 (1994).
32. R.M. Lin, M.K. Lim and H. Du, 'Deflection of plates with non-linear boundary supports using generalized differential quadrature', *Comput. Struct.*, **53**, 993–999 (1994).
33. R.M. Lin, M.K. Lim and H. Du, 'Large deflection analysis of plates under thermal loading', *Comput. Methods Appl. Mech. Eng.*, **117**, 381–390 (1994).
34. H. Du, M.K. Lim and R.M. Lin, 'Application of differential quadrature to vibration analysis', *J. Sound Vib.*, **181**, 279–293 (1995).
35. A.G. Striz, X. Wang and C.W. Bert, 'Harmonic differential quadrature method and applications to analysis of structural components', *Acta Mech.*, **111**, 85–94 (1995).
36. H. Du, K.M. Liew and M.K. Lim, 'Generalized differential quadrature method for buckling analysis', *J. Eng. Mech.*, **122**, 95–100 (1996).
37. C.W. Bert and M. Malik, 'Free vibration analysis of tapered rectangular plates by differential quadrature method: A semi-analytical approach', *J. Sound Vib.*, **190**, 41–63 (1996).
38. C.W. Bert and M. Malik, 'The differential quadrature method for irregular domains and application to plate vibration', *Int. J. Mech. Sci.*, **38**, 589–606 (1996).

39. A.R. Kukreti and J. Farsa, 'Differential quadrature and Rayleigh–Ritz methods to determine the fundamental frequencies of simply supported rectangular plates with linearly varying thickness', *J. Sound Vib.*, **189**, 103–122 (1996).
40. K.M. Liew, J.B. Han, Z.M. Xiao and H. Du, 'Differential quadrature method for Mindlin plates on Winkler foundations', *Int. J. Mech. Sci.*, **38**, 405–421 (1996).
41. C. Shu, 'An efficient approach for free vibration analysis of conical shells', *Int. J. Mech. Sci.*, **38**, 935–949 (1996).
42. C. Shu, 'Free vibration analysis of composite laminated conical shells by generalized differential quadrature', *J. Sound Vib.*, **194**, 587–604 (1996).
43. C. Shu and Y.T., Chew, 'Fourier expansion-based differential quadrature and its application to Helmholtz eigenvalue problems', *Commun. Numer. Methods Eng.*, **13**, 643–653 (1997).